

DEEP GEOLOGICAL BOREHOLES : A SUITABLE DISPOSAL ROUTE FOR THE HANFORD Cs/Sr CAPSULES?

Karl P Travis and Fergus G F Gibb

Department of Materials Science & Engineering, The University of Sheffield, Sheffield, UK S1 3JD.
k.travis@sheffield.ac.uk; f.gibb@sheffield.ac.uk.

The Hanford site in Washington State is the most contaminated site in the USA and presents a major environmental problem requiring clean-up. Just under 2000 prefabricated capsules containing halides of Sr-90 and Cs-137 and representing around 40% of the total radioactivity of Hanford high-level wastes (HLW) require a long-term disposal solution. Disposal in deep, geological boreholes has been suggested, as a safe, rapid and cost effective means of removing this substantial proportion of the radioactivity from the Hanford site.

In this paper we describe a physical model for disposal of all of the capsules in a single borehole. Numerical modeling is performed in order to solve the heat conduction equation, giving the spatial and temporal dependence of the temperature in the near-field. From the results of these finite difference calculations, we conclude that this disposal option is not only viable from the thermal loading point of view, but could be made even more efficient if a slightly wider borehole is considered, enabling a more dense packing of the capsules and their overpacks.

I. INTRODUCTION

The Hanford site in Benton County, Washington, was established in 1943 as part of the Manhattan Project, producing weapons grade plutonium in the B Reactor. It continued to be used to produce material for atomic weapons during the cold war before the onset of decommissioning operations. The legacy of this program is that the site is now the most contaminated in the USA presenting a major environmental and societal problem requiring clean-up.

Prefabricated capsules containing halides of Cs-137 and Sr-90 represent about 40% of the total radioactivity of Hanford HLW. There are 1935 of these capsules, each with a total length between 0.51 and 0.53 m and an outside diameter mostly of about 0.067 m. These capsules have a high initial thermal loading, though much of this will be exhausted over a time period of 200 years. All the Cs capsules also contain the longer-lived

Cs-135 isotope, with a half-life of 2.3 million years, presenting a long-term risk. Closure of the Yucca Mountain repository project in Nevada means that new solutions must be sought for the safe, long-term disposal of these and other HLWs at this site.

Geological disposal of HLW and used nuclear fuel (UNF) in very deep boreholes is a concept whose time has come. The alternative concept, being pursued by several countries including France, Sweden, Finland, Switzerland and the UK, and involving disposal in a mined underground repository, is beset with difficulties, not least of which are the constraints placed upon the engineered barriers by the high thermal loading. The deep borehole concept offers a potentially safer, faster and more cost-effective solution.

One suggestion is to dispose of the entire Hanford inventory of these capsules in a single deep geological borehole. The small diameter of the capsules plus overpack would require a relatively narrow borehole, easily attainable with current drilling technology. To explore the feasibility of this disposal option, we have conducted detailed heat flow modeling using the finite differences method. We describe our near-field modeling work in detail and show how temperature develops over time for strings of 10 two-capsule containers holding either Cs or Sr halide. We demonstrate that it is possible to dispose of the capsules in this way, and explore a more efficient disposal using larger containers and slightly wider boreholes.

II. DEEP BOREHOLE DISPOSAL

II.A. The Deep Borehole Disposal Concept

The deep borehole disposal (DBD) concept involves sinking a vertical hole to a depth of 4-5 km into the granitic basement of the continental crust. The hole is then lined with steel casing (perforated in the disposal zone) and the lower 1-2 km filled with waste containers together with a sealing and support matrix (e.g. bentonite clay). The remaining hole is then backfilled and sealed. Hole diameters in the disposal zone (DZ) can vary from

0.216 m to 0.610 m (Ref 4), but this is largely dependent on current drilling envelopes and the type of waste being considered.

While DBD is a multi-barrier concept, it puts the emphasis on an order of magnitude increase in the geological barrier compared to mined repositories such as SKB's KBS-3 concept. At the depths being discussed for DBD, lateral movement of groundwater is limited due to very low bulk hydraulic conductivities while upwards movement of potentially contaminated groundwaters is further constrained by a salinity gradient and density stratification. Apart from safety, speed of implementation is another major advantage offered by DBD over a repository; a single borehole could be drilled, cased, filled and sealed in a little over 3 years⁴.

DBD offers enormous flexibility in disposing of different waste inventories. A wide range of pre-packaged wastes can be dealt with by varying the diameter of the hole. Many DBD schemes for SF can accommodate complete used PWR and BWR fuel assemblies^{1, 4}. However the preferred option is consolidated disposal which offers an efficient means to dispose of a large number of spent fuel rods¹ in a single container compared to the disposal of complete fuel assemblies. A single borehole could contain waste packages consisting of combinations of old and young spent fuel for instance. Sealing and support matrices can be tailored to give the best possible performance for a given heat output; for example, the use of High Density Support Matrix² (HDSM) for spent fuel disposal offers potentially superior sealing of the waste packages against the saline groundwaters, while special cementitious grouts can be formulated with delayed setting times for use with lower heat content waste packages. With the ability to deliver the waste packages singly or in batches, DBD offers a one-stop-shop for safe, fast clean-up of pre-packaged wastes, provided the packages are not too large in diameter.

II.B. Baseline DBD concept for the Hanford capsules

The cesium and strontium capsules consist of a container in which cesium chloride or strontium fluoride is sealed within inner and outer steel walls. The capsules vary in length between 0.51 and 0.53 m, while their diameters range from 0.067 to 0.083 m.

The simplest borehole disposal concept for the capsules involves putting one, two or more of them end to end, axially aligned, inside a cylindrical disposal container (Fig. 1). As a "baseline" case, we have opted for two capsules base to base in a 1.083 m long stainless steel container (over-pack/canister) with an O.D. of 0.114 m and a wall thickness of 12.7 mm (Fig. 2). This would require a 0.216 m (8.5 in) diameter borehole and 0.178 m (7 in) O.D. casing. To minimise any risk of deformation or collapse under the disposal pressure and ensure

efficient conduction of decay heat away from the capsules the gap between the capsules and container should be filled with a high conductivity material such as lead or silicon carbide. The former has the advantages of being easy to pour into the gap when molten and of providing a degree of radiation shielding while the latter is cheap, lightweight and can be inserted as a dry powder or easily made into a sleeve or liner for the container. After insertion of the capsules any ullage should be filled and the container lid welded on. The annuli between the container and casing and between the casing and host rock should be filled or grouted but, given the relatively low weights of the packages and the likely strength of the containers, the fill or grout may not be required to function as a support matrix²⁻³. In other DBD concepts, e.g. for SNF, the fill or grout can also serve to protect the containers from premature corrosion by the highly saline groundwaters⁴ but in this case the relatively short half-lives of the main Cs and Sr radionuclides could enable this function of the fill also to be dispensed with. However, depending on the content of Cs-135, it may be desirable to prolong container life as much as possible. Possible fill or grout materials could include bentonite, cement and crushed host rock.

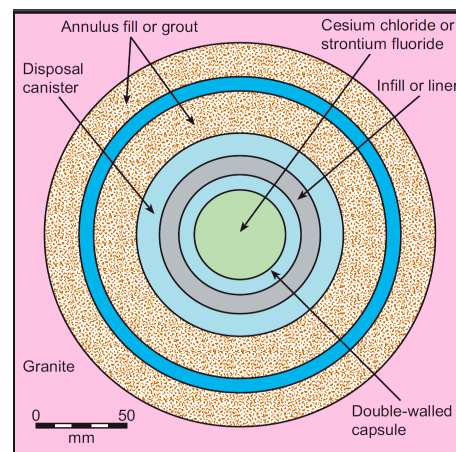


Fig. 1. Horizontal cross section of "baseline" DBD concept for CsCl and SrF₂ capsules. The outer (darker blue) ring is the casing.

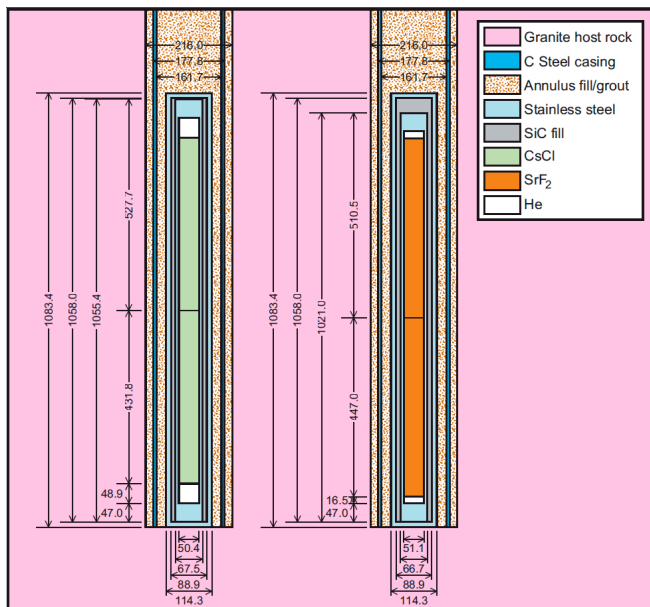


Fig. 2. Vertical cross sections of the “baseline” DBD concept as simplified for thermal modeling.

III. NUMERICAL MODEL AND SOLUTION

We restrict attention to the dominant heat transfer mechanism – conduction, in our heat flow modeling work (but see IV.C). The spatial and temporal variation of temperature is obtained as the solution of the heat conduction equation in cylindrical polar coordinates:

$$\frac{1}{R} \frac{\partial}{\partial R} \left(\kappa R \frac{\partial T}{\partial R} \right) + \frac{\partial}{\partial z} \left(\kappa \frac{\partial T}{\partial z} \right) = \frac{\partial T}{\partial t} - \frac{S}{\rho c} \quad (1)$$

where κ is the thermal diffusivity, ρ the density, c the specific heat, R is the radial coordinate, z is the vertical coordinate, while S is the volumetric rate of heat production. The thermal conductivity, $K (= \kappa \rho c)$ is taken to be piecewise constant; that is to say that within the spatial grid for a given material type, it has no spatial dependence.

Numerical solutions to eq. 1 have been obtained using the method of finite differences. We have employed the *GRANITE II*¹ code, for this purpose. We have decomposed the solution zone into several different material types, each with its own set of thermophysical properties. These are: the wall rock, mild steel borehole casing, stainless steel (for both the disposal container and capsule wall), bentonite (for the borehole filling material), and a material representing ‘waste’, which includes the source term (see below).

A rectangular mesh is then created using a non-uniform spacing; a finer spacing is employed in the near field environment, while a wider spacing applies further away from the container(s). The origin of the mesh is then placed along the axis of radial symmetry at the lowest part

of the first container emplaced down hole. A discretized version of eq. 1 can be written compactly using matrix notation. For a mesh consisting of n divisions along the radial direction and m divisions along the axial direction we have

$$\mathbf{A} \mathbf{T}^{t+\Delta t} = \mathbf{B} \mathbf{T}^{t+\Delta t} + \mathbf{S} \quad (2)$$

where \mathbf{T} and $\mathbf{T}^{t+\Delta t}$ are now column vectors containing the temperatures for the whole set of mesh points at the present time and the new time respectively, \mathbf{A} and \mathbf{B} are square matrices of dimension $n \times m$ that contain all the physical and geometrical parameters, while \mathbf{S} contains the contribution from the source and some of the boundary conditions. This is a fully implicit formulation. A lower/upper decomposition method with iterative refinement has been employed in the solution of this matrix problem.

The mathematical model is completed by the specification of the boundary conditions. These take the forms: (i) the conditions at the axis are that the temperature remains finite and that there is zero flux across this boundary $K \partial T / \partial R = 0$ at $R = 0$; (ii) at large distances from the source the temperature rise is set to be zero; (iii) at inter-regional boundaries it is ensured that the temperature and flux are the same on either side of the boundary; (iv) the initial condition takes a zero (or ambient) temperature over all spatial regions.

The top, middle and lower sections of the disposal container contents (Fig. 3) are each treated as if they were single composite materials with their thermophysical properties calculated as weighted averages of their actual contents. For each of the middle, heat generating sections, the radiogenic heat is distributed evenly over the cylindrical volumes depicted in Fig. 3, which include the steel capsule walls and SiC infill or sleeve. Densities and specific heats of all the composite materials (sections) are obtained using well-known mixing rules based on volume fractions (ϕ_i) and mass fractions (γ_i) respectively:

$$\rho_{tot} = \sum_i \phi_i \rho_i \quad (3)$$

$$c_{tot} = \sum_i \gamma_i c_i \quad (4)$$

where the subscript i refers to each individual component in the single composite material. For the thermal conductivities of a composite material (section), we use a simple thermal resistance model to combine the individual thermal conductivities. Considering the upper sections of the CsCl and SrF₂ disposal containers, the thermal resistance “circuit diagram” for each of these arrangements is shown in Figs. 4 -5 respectively.

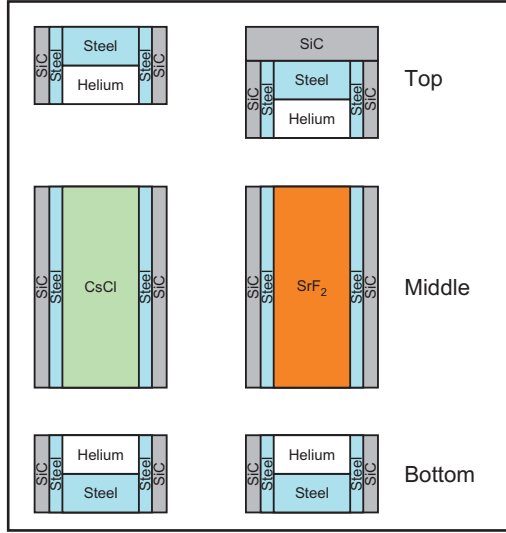


Fig. 3. Schematic diagram showing breakdown of material types in the two kinds of capsule: CsCl and SrF₂.

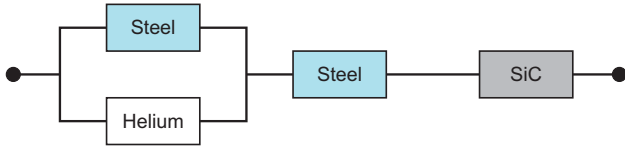


Fig. 4. Circuit diagram showing thermal resistances in series and parallel combinations for the CsCl source term.

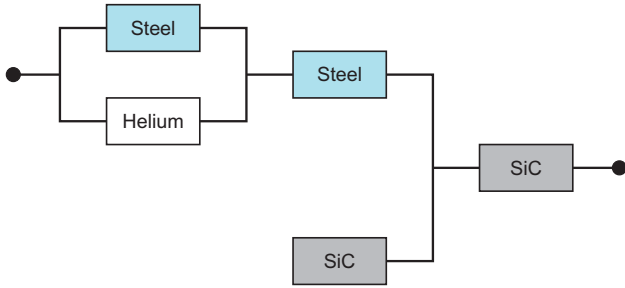


Fig. 5. Circuit diagram showing thermal resistances in series and parallel combinations for the SrF₂ source term.

The thermal conductivities of two thermal resistances in parallel are combined using a volume fraction weighted sum of their individual conductivities:

$$K_{series}^{-1} = \sum_i \phi_i K_i^{-1} \quad (5)$$

where the volume fractions refer to the volume of each component divided by the total volume of the two materials in the parallel section of the circuit. Thermal resistances in series are combined using the following equation:

$$K_{parallel} = \sum_i \phi_i K_i \quad (6)$$

Note that in the case of CsCl, there is a small (2.6 mm) gap between the top of the capsule and the inside surface of the container which would in reality be filled with SiC. In our modelling work we have ignored this tiny gap, instead treating the end cap of the capsule as if it were 2.6 mm thicker. For SrF₂, the gap is 37 mm and therefore too large to ignore. Consequently we have treated this case as if the capsule had an extra end cap made of SiC with a thickness of 37 mm (Fig. 3).

We have allowed for temperature dependent properties for all 8 material types used in the modelling work. Table 1 shows the ranges of properties used within the code (25°C – 250°C). These were either calculated from equations in the literature or, in cases where only tabulated data were available, are the result of polynomial fits.

Table 1. Thermophysical properties used in *GRANITE II* modelling.

	$\rho/(\text{kg m}^{-3})$	$c_p/(\text{J kg}^{-1} \text{K}^{-1})$	$K/(\text{W m}^{-1} \text{K}^{-1})$
CsCl	4003.5 – 3857.3	306.0 – 313.8	0.7808 – 0.4600
SrF ₂	2964.6 – 2924.8	399.5 – 450.5	4.223 – 2.567
Stainless steel	7900 - 7808	526.7 – 579.9	14.5 – 18.3
Helium [†]	0.164	5193.07	0.1505 – 0.2199
SiC	3100 - 3094	662.9 – 1002	333.6 – 149.7
Granite	2630.0	781.5 – 954.6	2.3 - 1.8
Carbon Steel	7860.0 – 7797.9	443.3 - 547.3	53.83 – 46.34
Bentonite	2010.0 – 1603.0	1330.0	1.15

[†] Helium properties refer to the thermodynamic state at 0.1 MPa and 20°C.

For the source term the data for SrF₂ and CsCl maximum and minimum heat outputs per container were fitted using cubic splines and then interpolated within the code. In all the models reported here, we employed a fixed time step of 400 s. Solutions were obtained for elapsed times of up to 1800 days.

IV. RESULTS AND DISCUSSION

IV.A. Heat conduction

The temperature measured at any point in or around the borehole will initially rise due to the

radiogenic heating from the waste packages but after reaching a maximum value, will slowly return to ambient as the activities of the halides within the capsules decay with time. It is of particular interest to determine the maximum temperature attained at any point and the time it takes to reach this temperature. We have modeled a stack of 10 containers (each with two halide capsules) and recorded the temperatures at 9 representative points that lie on the borehole axis, outer cylindrical surface of the containers, and the borehole wall at each of three levels (top, middle and bottom of the 10 container stack). We have considered two cases: a stack with containers comprising two capsules of SrF₂, and a second stack with containers of CsCl, both with the maximum initial heat output in the year 2020.

Figs. 6-7 show temperature-time curves for CsCl and SrF₂ respectively. The peak temperatures attained by the SrF₂ capsule stack are greater than those for the CsCl capsule case at all levels. For the top and bottom of the stack in both cases, the temperatures on the borehole axis and surface almost coincide due to the fact that the points lie in the stainless steel container material, which has a high thermal conductivity. Points on the borehole wall at the same level are several degrees cooler than on the container surface. Temperatures at the bottom of the stack are a few degrees hotter than those at the top; something which can be attributed to the less efficient downward conduction of heat (lack of steel casing and presence of rock below). The times taken to reach peak temperatures are similar for both halides (~ 1000 days).

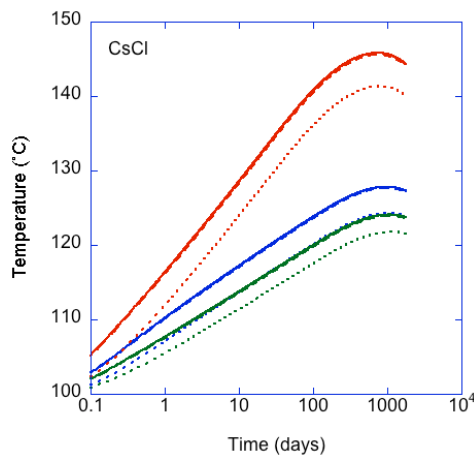


Fig. 6 Temperature vs time curves for a stack of 10 containers (two CsCl capsules in each) with maximum heat output. Curves are for points on the borehole axis (solid lines), the container surface (dashed lines) and the borehole wall (dotted lines). Blue = bottom; Red = middle; Green = top of the stack.

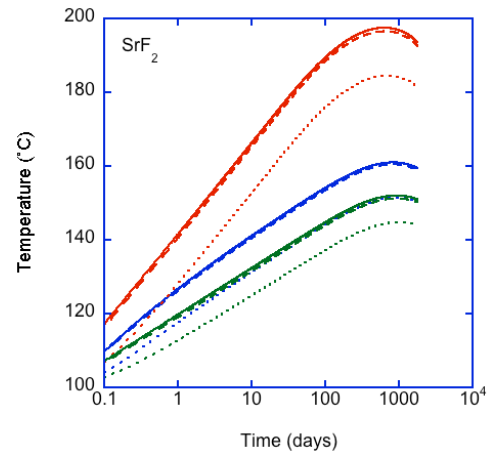


Fig. 7 Temperature vs time curves for a stack of 10 containers (two SrF₂ capsules in each) with maximum heat output. Key as Fig. 6.

Figs. 8-9 show the variation of peak temperature with height on the outer surface of the containers. The temperatures generated do not exceed 220 °C for SrF₂ and 160 °C for the CsCl. We have conducted a trial study using a stack of 50 containers and find that the peak temperatures for this 50 container stack do not go significantly higher than the 10 container values.

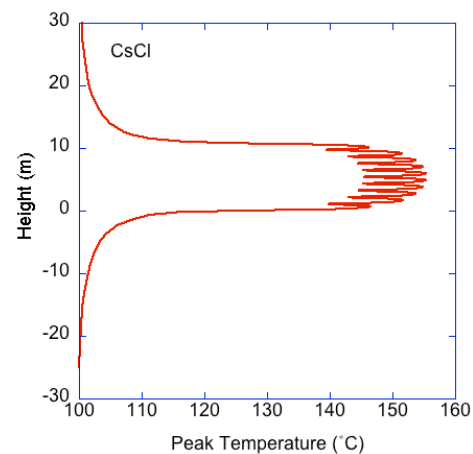


Fig. 8. Peak temperatures measured at the container surface as a function of height. 10 containers, each with two CsCl capsules and maximum heat output.

Figs. 10-11 show the variation of peak temperature along radii at the top, middle and bottom of a stack of 10 two-capsule containers. The greatest heats are generated just below the middle of the stack with temperatures at the top and bottom fairly similar. The most important information to draw from these diagrams is the radial distance at which the peak temperature drops to within 10 °C of ambient, which is within a few meters of the borehole axis in both cases. The thermal footprint of the borehole would therefore be quite small.

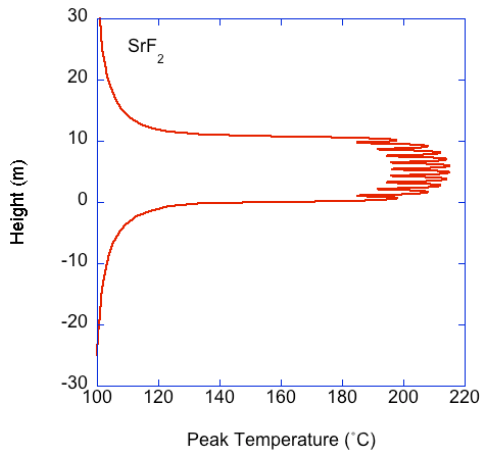


Fig. 9. Peak temperatures measured at the container surface as a function of height. 10 containers, each with two SrF₂ capsules and maximum heat output.

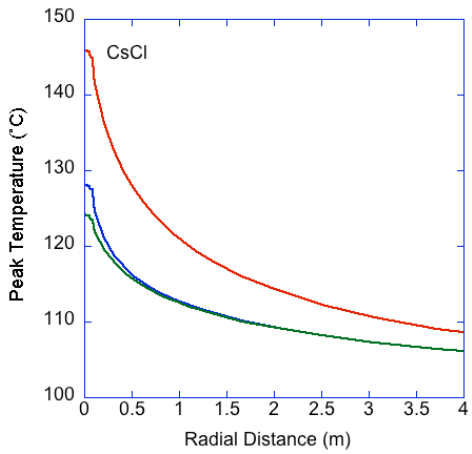


Fig. 10. Peak temperatures measured along radii perpendicular to the borehole axis at the top, bottom and middle of a 10 container stack. Colors as Fig. 6.

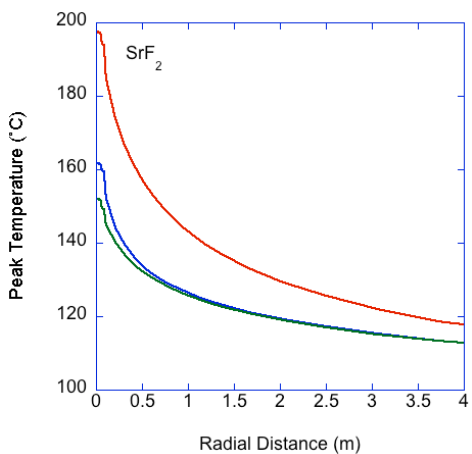


Fig. 11. Peak temperatures measured along radii perpendicular to borehole axis at the top, bottom and middle of a 10 container stack. Colors as Fig. 6.

IV.B. Convection.

The thermal modeling we have performed and described in the last section considered only the conductive flow of heat. Transport of heat by convection is not expected to be significant by comparison. However, convection could be important when considered as a possible mechanism for the upward transport of any radioactive species which may have entered the groundwater in and around the disposal zone. Two routes are possible: (1) convection taking place in the fluids within the borehole and particularly in the annulus between the wall and casing, and (2) convection involving host rock groundwaters. The first mechanism can be ‘engineered out’ through the use of mechanical borehole seals such as swell packers, or materials-based seals such as bentonite, asphalt or cement. It is essential that the annulus is sealed as well as inside the casing. This could be achieved either by withdrawing/cutting away the casing or filling it via the perforations. An estimate of the extent of transport via the second mechanism can be obtained using a simplified Darcy’s law model. Details on this calculation can be obtained from⁵. Briefly, Darcy’s law is solved in the Boussinesq approximation with the temperature change taken as that due to a steady point source of heat. The solution of this equation yields an expression for the vertical displacement of a particle, z ,

$$z = a \cosh \lambda \sinh \lambda \quad (7)$$

in which λ is a parameter which must be obtained from the implicit equation below

$$t = \frac{a^2}{C} \left[\frac{1}{2} \sinh \lambda \cosh^3 \lambda + \frac{3}{4} \sinh \lambda \cosh \lambda + \frac{3}{4} \lambda \right] \quad (8)$$

where t is time, and C is a parameter given by

$$C = \frac{\psi \beta q}{4\pi \kappa} \quad (9)$$

and for which ψ is the hydraulic conductivity, β is the thermal coefficient of volume expansion, q is the initial rate of heating ($S/\rho c$) and κ is thermal diffusivity. We have used the following values for our example calculation: $\beta = 0.00075 \text{ K}^{-1}$, $\psi = 10^{-11} \text{ ms}^{-1}$, $\lambda = 2.106 \text{ W m}^{-1} \text{ K}^{-1}$, $\rho = 2630 \text{ kg m}^{-3}$, and $c = 874.0 \text{ J kg}^{-1} \text{ K}^{-1}$, and a heat rate based on disposal of two SrF₂ capsules with the maximum heat output at the year 2020 ($S = 750 \text{ W}$). Calculations have been performed using three different values of the parameter a , (radial position when $z = 0$): 0.1 m, 1 m and 10 m and the results are plotted in Fig 12 for times up to 1 million years. From the figure it is apparent that a particle would move upwards by only 3 m at a radial position of 10 m and only 11 m upwards

within at a radial position of 0.1m. Convective transport through the host rock fluids is therefore negligible.

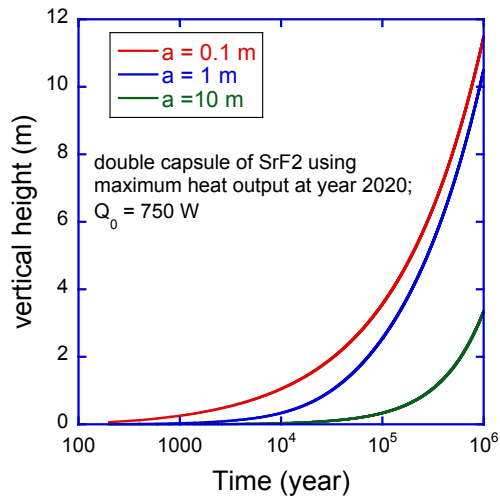


Fig. 12 Upwards displacement of a fluid particle calculated from the simplified Darcy law model and evaluated for 3 different starting distances (a) from the axis.

V. CONCLUSIONS

We have conducted thermal heat flow modeling in the near field of a single, 0.216 m diameter borehole filled with stacks of 10 containers, each with two capsules of either SrF₂ or CsCl at maximum heat output. Our results have been analysed in terms of temperature-time curves and plots of peak temperature versus radial distance or vertical height. These data show that a single borehole could be used to dispose of the entire Hanford capsule inventory with temperatures never rising high enough anywhere in or near the hole to prevent the use of standard sealing matrices, such as bentonite. However, far greater economy could be achieved if instead of putting only two capsules in the disposal container, we instead use 6 (in 2 rows of 3) or 14 (2 rows of 7) as indicated in Fig. 13. In order to achieve this greater packing, wider boreholes would need to be considered. However the increased cost of using a wider borehole would be offset by the use of a shorter disposal zone. The borehole diameters required for these two concepts (Fig 13.a and b) are still well within the envelop of existing drilling technology and experience.

Calculations have been undertaken to estimate the amount of upward vertical displacement of a contaminated groundwater particle that might occur due to convection through the saturated host rock. These calculations involved solving a Darcy's Law model and the results show that such upwards displacements can be disregarded (~3 m in a million years).

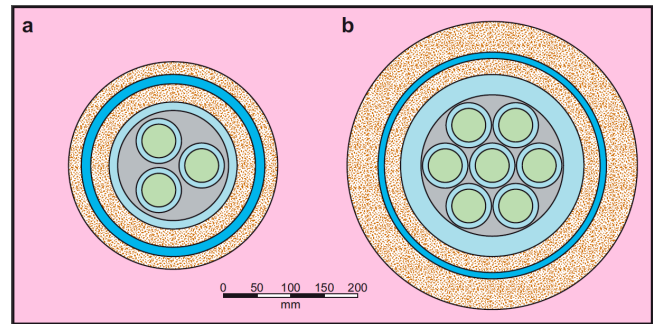


Fig. 13. Container geometries for possible alternative DBD concepts for CsCl or SrF₂ capsules. Colours as in Fig. 2

ACKNOWLEDGMENTS

We wish to acknowledge Sandia National Laboratories for the provision of data and helpful discussions during the course of this work.

REFERENCES

1. F.G.F. GIBB, K.P. TRAVIS AND K.W.HESKETH, "Deep borehole disposal of higher burn up spent nuclear fuels", *Mineralogical Magazine*, **76**, 3003 (2013).
2. F.G.F. GIBB, K.P. TRAVIS, N. A. MCTAGGART, and D. BURLEY "High-density support matrices: - key to the deep borehole disposal of spent nuclear fuel", *J. Nuc Materials*, **374**, 370 (2007).
3. B. W. ARNOLD, P. V. BRADY, S. J. BAUER, C. HERRICK, S. PYE AND J. FINGER, "Reference Design and Operations for Deep Borehole Disposal of High-Level Radioactive Waste", **SAND2011-6749**, Albuquerque, NM. Sandia National Laboratories (2011).
4. A. J. BESWICK, F. G. F. GIBB AND K. P. TRAVIS, "Deep borehole disposal of nuclear waste: engineering challenges", *Energy*, **167**, 47 (2014).
5. F.G.F. GIBB, K.P. TRAVIS, N. A. MCTAGGART, and D. BURLEY, "A model for heat flow in deep borehole disposals of high- level nuclear waste", *J. Geophys. Res. Solid Earth*, **113**, B05201 (2008).